Determination of the dispersion relation in cross-laminated timber plates: Benchmarking of time- and frequency-domain methods

Published Version:
Morandi F., Santoni A., Fausti P., Garai M. (2022). Determination of the dispersion relation in cross-laminated timber plates: Benchmarking of time- and frequency-domain methods. APPLIED ACOUSTICS, 185, 1-12 [10.1016/j.apacoust.2021.108400].

Availability:
This version is available at: https://hdl.handle.net/11585/835571 since: 2023-06-17

Published:
DOI: http://doi.org/10.1016/j.apacoust.2021.108400

F. Morandi, A. Santoni, P. Fausti, M. Garai,

Determination of the dispersion relation in cross-laminated timber plates: Benchmarking of time- and frequency-domain methods

Applied Acoustics, Volume 185, 2022

The final published version is available online at:

https://doi.org/10.1016/j.apacoust.2021.108400

Determination of the dispersion relation in cross-laminated timber plates: benchmarking of time- and frequency-domain methods

F. Morandi[a], A. Santoni[b], P. Fausti[b], M. Garai[c]

[a]*Faculty of Science and Technology, Free University of Bozen-Bolzano, Italy*
[b]*Department of Engineering, University of Ferrara, Italy*
[c]*Department of Industrial Engineering, University of Bologna, Italy*

Abstract

The availability of a reliable estimate of the dispersion relation of plates is of great importance for acoustic modelling. Several experimental methods for the extraction of wavenumber and wave velocity information are discussed in the literature. They differ, among other factors, by the sensitivity to noise and multiple reflections, frequency range of application and implementation of the processing algorithm. While for homogeneous thick or thin plates well-established analytical solutions are available, non homogeneous materials would benefit from experimental characterisation. In this framework, our attention is focused on cross-laminated timber (CLT) elements, load-bearing orthotropic layered wood plates that revolutionised the sector of timber construction. The anisotropic and non homogeneous nature of wood suggested testing methods that, though converging for homogeneous materials, could bring different results in their application to CLT elements. The aim of this paper is therefore to benchmark methods for the extraction of wavenumber information on CLT plates, from which the effective elastic properties to model CLT structures as an equivalent homogeneous plate can be derived. This is achieved through a numerical and experimental benchmark of well-established methods for the evaluation of the real component of the propagating wavenumber in CLT elements. Five relevant methods were selected through a literature review, implemented and analyzed: three in the time domain, namely maximum peak, cross-correlation and kurtosis, and two in the frequency domain: phase difference and wave correlation. First, the five methods were benchmarked by numerical simulation on a homogeneous material. In this ideal case, results showed to be consistent for all methods. Then, wavenumber measurements were performed on a cross-laminated timber plate. The results show that the maximum peak, cross-correlation and the wave correlation method provide the lowest dispersion of the data. Considering the time required by the installation of the setup, the wave correlation method seems to be the best alternative among the proposed ones.

Keywords: Structural acoustics, wave propagation, dispersion relation, cross-laminated timber

1. Introduction

Cross-laminated timber (CLT) is a engineered-wood product made of layers of timber planks glued crosswise. The product was originally developed in the late 1990s with the aim of using cuts that could not be used otherwise for structural products and it integrates the set of available wood engineered products [1]. CLT elements are bi-dimensional products characterised by a high out-of-plane stiffness; the alternation of crossed layers also allows to compensate for shrinkage effects, which are much more evident in products made of layers with equally oriented strands. The diffusion of CLT has allowed the wood construction market to develop integral timber construction systems also for large volumes/high rise constructions. In hybrid high-rise timber constructions, CLT is used for floors, shear walls and vertical-loads carrying elements. In-depth research has been conducted to investigate seismic behaviour, thermal insulation and fire resistance of CLT elements [2, 3, 4, 5]. The evolution of the construction sector, moving towards prefabrication, is seeking solutions for shortening construction time and higher quality standards. Thanks to the reduced weight, wood elements are a natural choice to produce highly prefabricated components and the whole wood construction market is expected to see a relevant increase in volume in the forthcoming years [6]. Timber construction plays a relevant role in meeting the goal of decarbonisation of the construction sector. Its eco-friendly environmental footprint can be traced back to several factors: first, the production of the raw material has a low environmental impact compared to traditional construction materials - also without considering the CO2 stored by the trees during growth [7]. Then, a turning point is represented by the transition from the concept of “extraction” to the concept of “growth” of the natural resource [8]. Finally, another environmental benefit associated with the construction process of timber buildings is represented by the reduced emission of particulate matter during construction [9].

Acoustics, ultrasonic, and vibro-acoustics measurement techniques are widely used throughout the whole wood value chain for the estimate of the elastic properties of wood and for the detection of damage. Sonic and ultrasonic testing, together with vibration-based testing, are techniques commonly used to assess properties of timber elements (such as MOE and moisture content), or the presence of damage such as delamination or defects [10, 11, 12, 13]. In particular, ultrasonic testing is one of the most common methods used for timber grading (see, for instance, [14]), together with modal testing (see, for instance, [15]). As previously mentioned, CLT elements in high-rise multi-unit residential buildings built using a hybrid building technology are mainly used to load bearing walls and floors. It is then straightforward that an in-depth knowledge of acoustic modelling of sound radiation of such elements is important to guarantee the health and comfort requirements in terms of sound insulation. Sound radiation is a phenomenon associated to the vibration of a plate coupled with wave propagation in the adjacent fluid, air in our case. Radiation is governed by flexural waves, which are dispersive: the evaluation of the structural wavenumbers freely propagating in a given structure is a key information regarding its dynamic behaviour. ~~The accurate estimate of the structural wavenumber also allows for the identification of the coincidence frequencies, and therefore to distinguish between the three regions marked by the critical frequency, characterised by different radiation efficiencies.~~ Assuming the equation of motion of the structure to be known, the experimental wavenumber, or wave velocity dispersion relation, allows for a complete characterisation of the elastic and damping properties of the material [16]. The wavenumber dispersion relation can be used to identify the elastic constants of a homogeneous element, or to determine a set of apparent effective elastic properties, which can also be frequency-dependent, of a structure with a rather complex dynamic behaviour (eg. such as laminated or sandwich elements) [17, 18], in order to approximate its vibro-acoustic response by using the simple theories for thin or thick plates.

~~The flexural wavenumber can be modelled or measured.~~ Several experimental methods exist to extract wavenumber information, which, according to Margerit et al. [19], can be classified in relation to four features: robustness, frequency range of application, ability to detect angle-dependent features and ability to return real or complex wavenumbers. Another factor of discrimination is the input data required for the implementation of each method. The ease of the measurement procedure is also a factor to consider [20]. While dealing with ideal, homogeneous and isotropic plates, modelling and measurements converge. Also the differences between different measurement and signal processing methods agree. Conversely, dealing with non homogeneous and non-isotropic materials, discrepancies arise between modelling and measurements, and also between measurement techniques. For what concerns CLT structures, both resonant and broad frequency-based, as well as time-based methods to investigate their elastic properties, can be found in the literature. For example Steiger et al. [21] and Gsell [22] et al. presented experimental methods to determine the elastic properties of CLT structures considered as an equivalent homogeneous orthotropic panel. Van Damme et al. [23, 24] performed experimental testing on CLT beams in order to determine structural elastic properties through a comparison of the experimental bending resonance and value resulting from either the classic theory for thin beams or the Timoshenko theory for thick beams. Santoni et al. [16] proposed an experimental method based on wave velocity identification to determine the frequency-dependent elastic properties of a CLT plate, by evaluating either the time delay or the phase difference between a pair of signals. A quick procedure to extract wavenumber information and thus to retrieve the elastic constants of CLT panels was presented by Thies et al. [25], showing preliminary results of an experimental analysis conducted on several CLT panels, characterised by different thickness and orthotropic ratios. These results were compared with the elastic parameters provided for structural calculations.

This paper does not want to provide an extensive literature review of the different non-destructive methods available to investigate the elastic properties of CLT elements. It rather aims at identifying which methods are more suitable to be used for the assessment of flexural wavenumber propagation, within a frequency range adequately extended in order to evaluate effective elastic properties of CLT elements, which are inhomogeneous, non-isotropic layered structures. Five representative methods which can be applied within the acoustic frequency, were firstly benchmarked using a numerical dataset obtained from Finite Element (FE) simulations on a isotropic homogeneous structure. Then they were applied for the experimental evaluation of the dispersion curves of a CLT panel.

The paper is organised as follows. The next section expresses the motivation for this work, and why it is often necessary to adopt homogenised models for a vibro-acoustic analysis of CLT systems. The theoretical background on bending wave propagation for thin and thick plates is provided in Section 3, together with the description of the methods considered in the present study. Section 4 benchmarks the different methods using numerical input data, to assess how each method performs under optimal conditions. Section 5 presents the test facilities and the techniques used to acquire the experimental input data. The data processing procedure and the experimental results are presented in Section 6. For each method, the outcomes of the experimental application are analyzed in relation to the numerical one. Furthermore, strengths and weaknesses of the methods are discussed. The main outcomes of this work are finally summarised in the conclusions.

2. Motivation and method

~~Knowledge of dispersion relations of CLT building elements is relevant for the modeling of their vibro-acoustic behavior as it allows to estimate the plate's elastic properties, damping, and coincidence frequencies.~~ CLT proves to be a challenging benchmark for comparative testing because of the peculiar mechanical properties of wood. Wood is an anisotropic and inhomogeneous material; CLT panels, due to their production process, very often exhibit a highly orthotropic behaviour. Several attempts to model the structural and the vibro-acoustic behaviour of CLT elements can be found in the literature. Qian et al. [26] recently presented an FE-based prediction tool to quantify the uncertainty induced in vibro-acoustic modelling of CLT structures by the material properties. Due to the complexity of CLT systems, they were often approximated to an equivalent homogeneous element. For example Fürtmuller et al. [27] proposed an FE approach to derived equivalent mechanical properties to investigate the structural behaviour of CLT components treated as shell elements. Santoni et al. [28, 29] presented prediction methods to evaluate the resonant radiation efficiency and the transmission loss of CLT panels considered as an equivalent thin orthotropic plate and characterised by frequency-dependent elastic properties. Higher order plates theories were considered in order to improve the modelling of shear deformation, both from a structural point of view [30], as well as a vibro-acoustic one [31]. Yang et al. [32] recently presented a wave and finite element approach to investigate the vibro-acoustic behaviour of CLT panels either by modelling each layer as a homogeneous orthotropic material, or by considering the panel as a single layer of an equivalent homogeneous orthotropic material. ~~The identification of wavenumber dispersion relation of a CLT panel allows to obtain information about the dynamic behaviour of the structure, which can be used either to describe it as an equivalent homogeneous element, or to determine its elastic properties through a best fitting of the experimental data with an analytical dispersion relation.~~ The identification of the wavenumber dispersions relation of a CLT panel is relevant for its vibro-acoustic modelling. In fact, these can be used to evaluate effective elastic properties to treat the CLT structure as an equivalent homogeneous element, and to approximate its vibro-acoustic behaviour by means of simplified plates theories. The accuracy of vibro-acoustic simulations based on either the classical plate, or the first order shear deformation theories, rather than on the three-dimension elasticity model, were discussed by Arasan et al. [33]. As already mentioned, this contribution aims at providing a comparative assessment of five measurement methods, which, according to the authors, are among the best suited for the identification of the dispersion curve of CLT structures, within the acoustic frequency range. This will be useful for researchers and engineers looking for a suitable tool to determine the effective elastic properties of CLT structures, to be used as input data in vibro-acoustic simulations.

Methods implemented in the time domain and in the frequency domain were chosen, requiring different measurement setups, showing different computational times and robustness to non-ideal propagation characteristics of media. The comparison was first conducted through a benchmark on numerical simulations performed with FE models. Then, the same methods were tested on experimental measurements performed on a CLT plate. The investigation therefore seeks to benchmark different methods for the extraction of wavenumber information, whose reliability was previously assessed on a numerical data set, through the use of real measured data with the aim of identifying the algorithm and measurement technique that is better suited for CLT elements. Through a thorough analysis of the outcomes and drawbacks of each method, the results mean to provide indications on how to approach these structures and to reduce the uncertainties that wrong estimates of k have on calculation methods.

3. Theoretical background

In classical plate theory, there is a distinction between 'acoustically' thin and thick plates. When $\lambda_B > 2\pi h$, being λ_B the flexural wavelength and h the thickness of the plate, shear deformation and rotational inertia can be neglected and the plate can be modeled as thin. Thin plates are modeled according to the Kirchhoff-Love theory [34] and the dispersion relation follows:

$$c_K = \sqrt{\omega}\sqrt[4]{\frac{Eh^2}{12\rho\,(1-\nu^2)}} \tag{1}$$

where c_K is the bending wave velocity (thin plates), ρ is the density of the plate, h its thickness, ω is the angular frequency, E the elastic modulus and ν Poisson's ratio.

The formulation of the governing equation for thick plates, accounting for shear deformation and rotatory inertia, was derived in the 1950s by Mindlin. The dispersion relation hence becomes [35]:

$$\left(1 - \frac{c_M^2}{T^2 c_S^2}\right)\left(\frac{c_L^2}{c_M^2} - 1\right) = \frac{12}{h^2 k_K^2} \tag{2}$$

where c_M is the bending wave velocity (thick plates), c_S is the shear wave velocity, c_L is the longitudinal wave velocity, h is the thickness of the plate and k_K is the wavenumber computed from the bending velocity given in Eq. (1).

To consider that the shear stress is not constant over the plate cross-section, the coefficient T is given as the ratio between the Rayleigh surface c_R wave velocity and the shear wave velocity c_S, and can be computed as [36]:

$$T = \frac{c_R}{c_S} = \frac{0.87 + 1.12\nu}{1 + \nu} \tag{3}$$

The longitudinal and the shear wave velocities can be described as:

$$\begin{aligned} c_L &= \sqrt{\tfrac{E}{\rho(1-\nu^2)}} \\ c_S &= \sqrt{\tfrac{G}{\rho}} \end{aligned} \tag{4}$$

where G represents the shear modulus.

For thin plates, the velocity of bending waves is proportional to the square root of the frequency. The dispersion curve for thick plates follows an asymptotic behavior; at low frequencies it behaves according to the thin plate theory, while at higher frequencies it approaches asymptotically the velocity of shear waves. Rindel [37] provided a simplified relation that describes the propagation of bending waves as a combination of the velocity of bending waves according to Kirchhoff-Love theory and the velocity of shear waves:

$$c_{B,eff} \approx \left[\frac{1}{c_K^3} + \frac{1}{c_S^3}\right]^{-1/3} \tag{5}$$

From the wavenumber dispersion curve it is possible to evaluate the elastic properties of the investigated structure by assuming an analytical dispersion relation. A non-linear fit of the experimental wavenumbers, with the chosen dispersion relation, would provide the elastic properties of the investigated structure. When rotatory inertia and shear deformation have a negligible influence on the structural response, the wavenumber dispersion relation based on Kirchhoff's thin plate theory can be derived from Eq. (1). However, when the structural wavelength is of the same order of magnitude as that of the thickness of the structure, shear deformation and rotary inertia have to be considered, otherwise the results will be misleading. In this case, Mindlin's wavenumber dispersion relation for thick plates should be used. This is analogous to Eq.(2), which express the dispersion relation in terms of wave velocity. By using Eq.(2), expressed in the wavenumber domain, it is possible to determine both the modulus of elasticity E and the shear modulus G, when the latter affects the dynamic behaviour of the investigated structure; otherwise, if the influence of shear deformation is negligible, the fitting procedure would still provide an accurate elastic modulus E even though a non reliable shear modulus G would also be found, as discussed in the next section.

The methods that can be used for the determination of the wavenumber can be categorised as time-domain methods and frequency-domain methods. In the following, the five methods considered are briefly described.

3.1. Time domain methods

Time domain methods are based upon the determination of the Time-of-Flight (ToF), i.e. the time lag characterizing the acquisition of a signal by two sensors separated by a known distance. Natural applications of these methods are in the mid-high frequency range, because of the limitations arising due to the distance between the sensors in relation to the investigated wavelength. In fact, time domain methods are commonly used in the ultrasonic frequency range, where the accuracy of the onset detection is of paramount importance [38]. The velocity of wave propagation in the time domain is usually measured through the analysis of a wave packet in order to minimise the dispersion effects and to easily window out unwanted reflections.

3.1.1. Maximum peak

The most common method for the determination of the ToF is the identification of the maximum peak of the signal. Considering a pulse centered on a known frequency and recording the signal at two positions, aligned with the source and having a mutual distance d, the time signal recorded by the second accelerometer will be attenuated and time-delayed with respect to the first one. Identifying the arrival time of the absolute maximum of the pulse at the two positions, the time difference t will provide a direct estimate of the ToF [39]. The velocity of the propagating wave c can be finally evaluated through the relation $c = d/t$. If multiple pulses are generated at different frequencies, the dispersion curve can be built frequency by frequency. The frequency range of application of the ToF algorithm based upon the detection of the maxima is related to the distance between the receivers. At low frequencies, when the wavelength is greater than the distance between the accelerometers, this method cannot be used. For low frequencies, the dispersion curve is often calculated with the phase difference between the two signals. The frequency limit that devises the phase and the ToF approach cannot be calculated *a priori* because the phase velocity is unknown. Thus, both methods are often implemented on overlapping frequency ranges around the guessed limit frequency. Most of the limitations related to the use of this method are the robustness problems arising when the signal-to-noise ratio (SNR) is low and when multiple reflections generate interference.

3.1.2. Cross-correlation

Cross-correlation is another well-known technique for the estimation of the ToF. Two signals s_1 and s_2 are recorded by accelerometers spaced at a distance d. The signals are cross-correlated, i.e. they are shifted one with respect to the other and their product is summed term by term:

$$(s_1 \star s_2)(\tau) = \int_{-\infty}^{\infty} s_1^*(t) s_2(t+\tau)\, dt \tag{6}$$

where * denotes the complex conjugate. When the signals are aligned, the cross-correlation function assumes a maximum at a lag τ that corresponds to the ToF. Dividing the distance d by the ToF, a direct estimate of the wave velocity can be obtained [40]. The accuracy of this method depends upon the width of the correlation peak, providing better estimates when narrow. This method is quite sensitive to multiple early reflections [41], therefore only the direct field should be analyzed. The correlation approach is also at the base of the Wigner-Ville analysis, used to extract wavenumber information [42].

3.1.3. Kurtosis

The kurtosis is the fourth order cumulant of a distribution; it measures how much the probability distribution of a variable differs from a normal distribution. Since the kurtosis of a normal distribution equals 3, it is common to describe the normalised kurtosis as:

$$\mathcal{K} = \frac{X(x-\mu)^4}{\sigma^4} - 3 \tag{7}$$

where X is the expected value, μ is the mean value of the series and σ is the standard deviation. Assuming that measured noise is Gaussian, the normalised kurtosis calculated on a running window will assume a value of zero. When the direct sound arrives, the tail of the distribution changes rapidly and the kurtosis increases rapidly. Thus the arrival of the direct sound is related to the point in which the kurtosis reaches a maximum. Thus, taking the corresponding time of the direct path, the phase velocity can be evaluated [43]. Unlike classical ToF methods, a high order cumulant such as the kurtosis contains amplitude and phase information and therefore provides an interesting advantage in the determination of the onset of a signal [44]. For the application of the kurtosis method, the most relevant step is the correct choice of a suitable time window to run over the signal and on which to compute the kurtosis.

3.2. Frequency domain methods

Several alternative methods can by used in order to characterise elastic or visco-elastic materials [45], which, unlike the approaches introduced so far, are applied in the frequency domain rather than in the time domain. While time domain algorithms generally use single frequency pulses, frequency domain measurements are generally performed using broad band exciting signals. Some of them, based on resonant techniques, allow to evaluate the elastic properties associated to the resonant frequency of the measured dynamic response [46, 23], while other methods allow to directly determine the dispersion curve either in terms of the propagating wave velocity or in terms of wavenumbers [24, 47].

3.2.1. Phase Difference

The phase velocity of lateral displacement can be determined by evaluating the phase difference between a pair of adjoining transducers. Therefore, even though this method deals with signals in the frequency domain, its application is very similar to the time-domain based methods previously described. The dynamic response of the investigated structure is in fact evaluated on pairs of positions. A fast Fourier transform (FFT) is performed on the signals, conveniently windowed to consider only the direct incoming wave [48], in order to obtain magnitude and phase in the frequency domain. The real part of the flexural wavenumber Re (k_B) can be evaluated and averaged over n measurement positions as:

$$\mathrm{Re}\left\{k_B(\omega)\right\} = \frac{1}{n-1}\sum_{i=1}^{n-1}\left(-\frac{\Delta\phi_{i,i+1}}{\Delta d_{i,i+1}}\right), \tag{8}$$

where $\Delta\phi$ represents the phase difference between two measured signals and Δd the mutual distance between corresponding sensors.

3.2.2. Wave Correlation method

Wave-correlation approaches require the evaluation of the dynamic response of the investigated structure, usually due to a broadband excitation, along a line, or over a grid of equally distributed points. A spatial Fourier transform (SFT) can be applied to the dynamic response $w(\omega, x)$ in order to obtain its spectrum in the wavenumber domain $w(\omega, k_x)$.

The length L_e over which the structure dynamic response is measured determines the lower frequency limit for wavenumber extraction, according to the relation: $L_{e,min} \geq \lambda(f_{min})/2$. The spacing between measurement points determines the maximum wavenumber that can be evaluated according to the Shannon-Nyquist theorem criterion: $k_{max} < \frac{\pi}{2\Delta x}$.

When the investigated structure has clamped boundary conditions, a zero-padding is usually applied to the measured response, artificially increasing the wavenumber resolution [24, 49]. Alternatives to the SFT, to perform transformation of the measured structural response from the spatial domain to the wavenumber domain, were discussed by Roozen et al. [50].

For example, a correlation function can be computed between the measured dynamic response $s(\omega, x)$ and a propagating inhomogeneous plane wave $o(\omega, k_x)$, as proposed by Berthaut et al. [51] and by Ichchou et al. [52, 53].

The 1D inhomogeneous plane wave is defined as: $o(\omega, k_{x,r}, k_{x,i}) = \exp(\pm j k_{x,r} x + k_{x,i} x)$, where $k_{x,r}$ is the real part of the complex wavenumber $\tilde{k}_x$, while $k_{x,i}$ represents its imaginary component, associated with the damping of the system. In this study, a mono-dimensional plane wave was considered, although this methods allows also to address propagation in two dimensions. Moreover, variations of this method have been proposed to overcome the far field assumption, allowing for example to consider the dynamic response close to the excitation point, where the plane wave assumption does not approximate well the actual vibration field, or to include the effect of reflections [54, 55].

For each investigated frequency, the structural wavenumbers were determined by maximizing the function:

$$\mathcal{F}(\omega, k_x) = \frac{\sum_n s(\omega, x)\, o^*\left(\omega, \tilde{k}_x\right) \Delta x}{\sqrt{\sum_n |s(\omega, x)|^2 \Delta x \sum_n \left|o\left(\omega, \tilde{k}_x\right)\right|^2 \Delta x}} \tag{9}$$

where Δx represents the spacing between two adjacent measurement positions, expressed in meters, s is the spatial response, and the symbol $*$ represents the complex conjugate.

4. Benchmarking of methods

In order to evaluate the reliability and the accuracy of the five chosen methods and, more specifically, of their implementation, a preliminary benchmarking was performed on an ideal numerical data set, not affected by a poor signal to noise ratio, nor by reflections due to discontinuities of the real structures, nor to experimental errors. To this purpose, FE models were implemented to investigate structural wave propagation in a homogeneous isotropic element, for which both the elastic constants and the wave velocity dispersion relation are well defined. The models were implemented using the *structural mechanics module* of the commercial software Comsol Multiphysics. A time dependent analysis was performed on a 2 m long, 0.5 m wide and 0.012 m thick plasterboard, with density $\rho = 840$ kg/m^3, Young modulus $E = 2.80$ GPa, Poisson's ratio $\nu = 0.33$, and internal loss factor $\eta = 0.05$. The structure was modelled as a 3D elastic solid. A structured quadrilateral mesh was adopted, with maximum size smaller that 1/6 of the shorter investigated wavelength. At one end of the board, a Gaussian pulse, generated at different frequencies, was imposed as prescribed displacement, while a fixed boundary condition was applied to the other end. The dynamic response of the excited board was evaluated on ten pairs of points equally spaced ($\Delta x = 50$ mm). The propagation velocity of the flexural wave was thus evaluated by processing each couple of numerical signals by means of the methods described in section 3.1. A frequency-domain analysis (considering a harmonic condition) was also performed on the same model, in order to investigate the structural wavenumbers propagating into the plasterboard. A broad-frequency excitation was applied as boundary load to one end of the investigated board and the excitation frequency was swept from 20 Hz to 5000 Hz at steps of 10 Hz. Moreover, in order to investigate the influence of shear deformation and rotatory inertia, boards with a different thickness were considered: 12 mm, 24 mm, 48 mm, 96 mm. The propagating wavenumbers were determined, according to the approach described in section 3.2.2, from the dynamic response evaluated over evenly distributed points with spacing Δx.

The results of the wave velocity obtained from the four presented ToF-based approaches, averaged over ten pairs of evaluation points, are compared in Figure 1 with the theoretical dispersion relation for bending waves. Figure 1d) also reports the wave velocity obtained from the phase difference method, described in section 3.2.1, given that the output of this method is analogous to and comparable with the results of ToF-based methods. In fact, even though it can be categorised among the approaches developed within the frequency domain, single frequency pulses are excited into the investigated structure, rather than a broadband signal. These four methods provided reliable results, in perfect agreement with the bending wave velocity computed using Eq. (1). The highest variability, expressed in the graphs in terms of standard deviation by the bar errors, was always found at the lowest investigated frequency, irrespective of the adopted method. It can be observed that each of these methods can provide accurate results, at least when applied to numerical and noiseless signals. However, it should be mentioned that each processing algorithm is sensitive to different parameters which need to be conveniently tweaked, according to the investigated frequency, in order to properly compare the two signals: for example, the criteria to identify the same peak of the propagating pulse or the size of time window which has to be applied in order to avoid influence of reflections. From the average value of the propagation velocity, the elastic modulus of the plasterboard element was evaluated according to Kirchhoff's dispersion relation. The results obtained from the different methods are summarised in Table 1 and compared with the target value, represented by the elastic modulus used as input data in the FE model: $E = 2.80$ GPa.

The structural wavenumbers obtained from the frequency-domain FE model for each investigated element are compared in Figure 2 with the dispersion curves for thin and thick plates, given in Eq. (1) and (2) respectively. The board's dynamic response was evaluated on a line of equally spaced points, aligned with the excitation force.

As mentioned in Section 3.2.2, the upper limit in the wavenumber domain is dependent upon the distance Δx between two adjoining evaluation points. This effect is highlighted in Figure 2: a spacing of $\Delta = 50$ mm, determined the upper wavenumber limit, $k_{max,\Delta=50mm} \approx 31$ rad/m, which is reached at frequencies around $f = 1000$ Hz in the 12 mm thick beam, $f = 1800$ Hz in the 24 mm thick beam, $f = 3000$ Hz in the 48 mm thick beam, and $f = 4200$ Hz in the 96 mm thick beam. On the other hand, reducing the distance between the evaluation points to $\Delta x = 10$ mm allowed to accurately approximate the propagating wavenumber in the entire frequency domain, since $k_{max,\Delta=10mm} \approx 157$rad/m. The wavenumber resolution δk is associated to the evaluation length L_e, i.e. the span covered by the array of measurement points: $\delta k = 2\pi/L_e$. The first evaluation point was chosen at 50 mm from the point load while the last position was evaluated at 50 mm from the opposite end, resulting in an evaluation length L_e= 1.8 m, which determined a wavenumber resolution: δk= 3.5 rad/m. As shown in Figure 2, as the thickness of the investigated structure increases, the dispersion relations for thin and thick plates increasingly deviate, since shear deformation and rotatory inertia have a greater influence. The elastic moduli of the investigated structures, obtained from the wave correlation method, are listed in Table 1. It is clear that, as the thickness of the element increases, the thin plate dispersion relation fails to

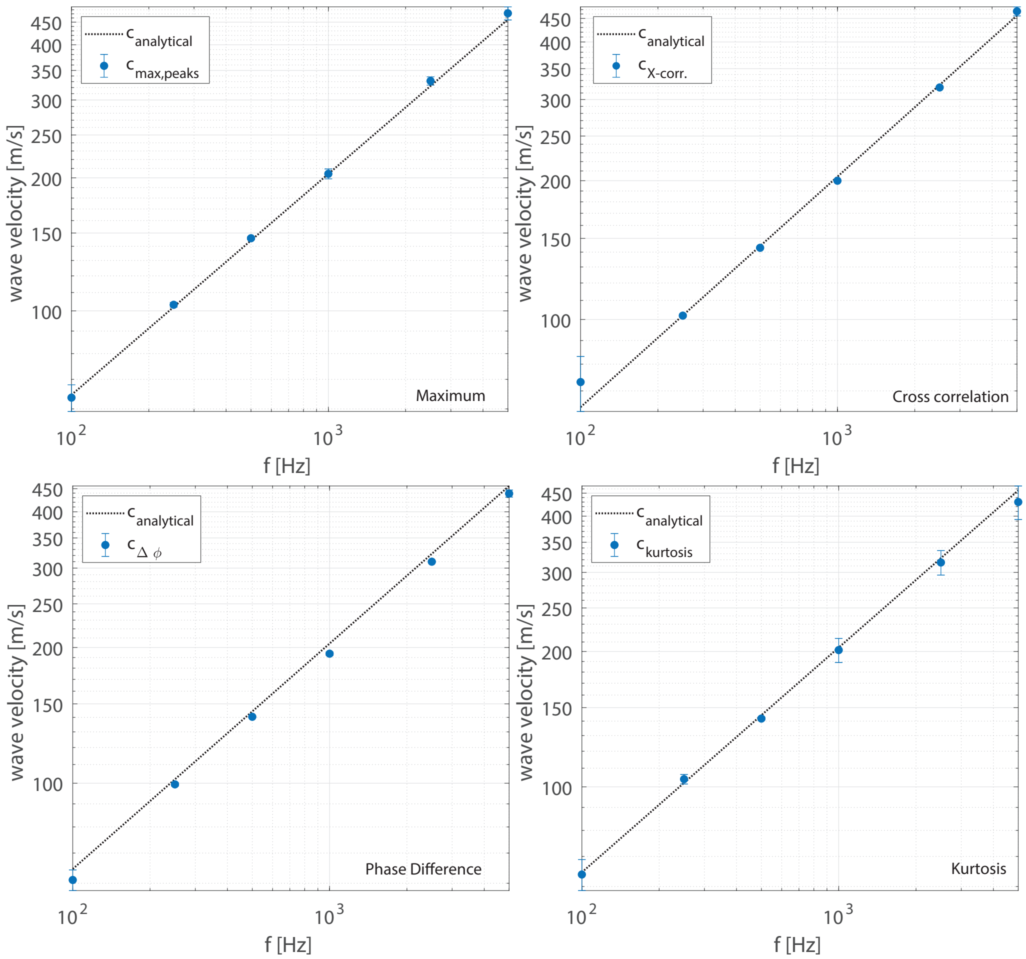

Figure 1: Benchmark results: comparison between the analytical dispersion curve for bending waves and the wave propagation velocity evaluated from time domain FE simulations.

evaluate the elastic modulus since the influence of shear deformation and rotatory inertia cannot be neglected. On the other hand, Mindlin's dispersion relation is suitable to accurately determine the elastic properties both for thin and thick elements. Moreover, the shear modulus can also be accurately evaluated if the investigation is performed up to high frequencies, where it has a significant influence on the structure's dynamic response.

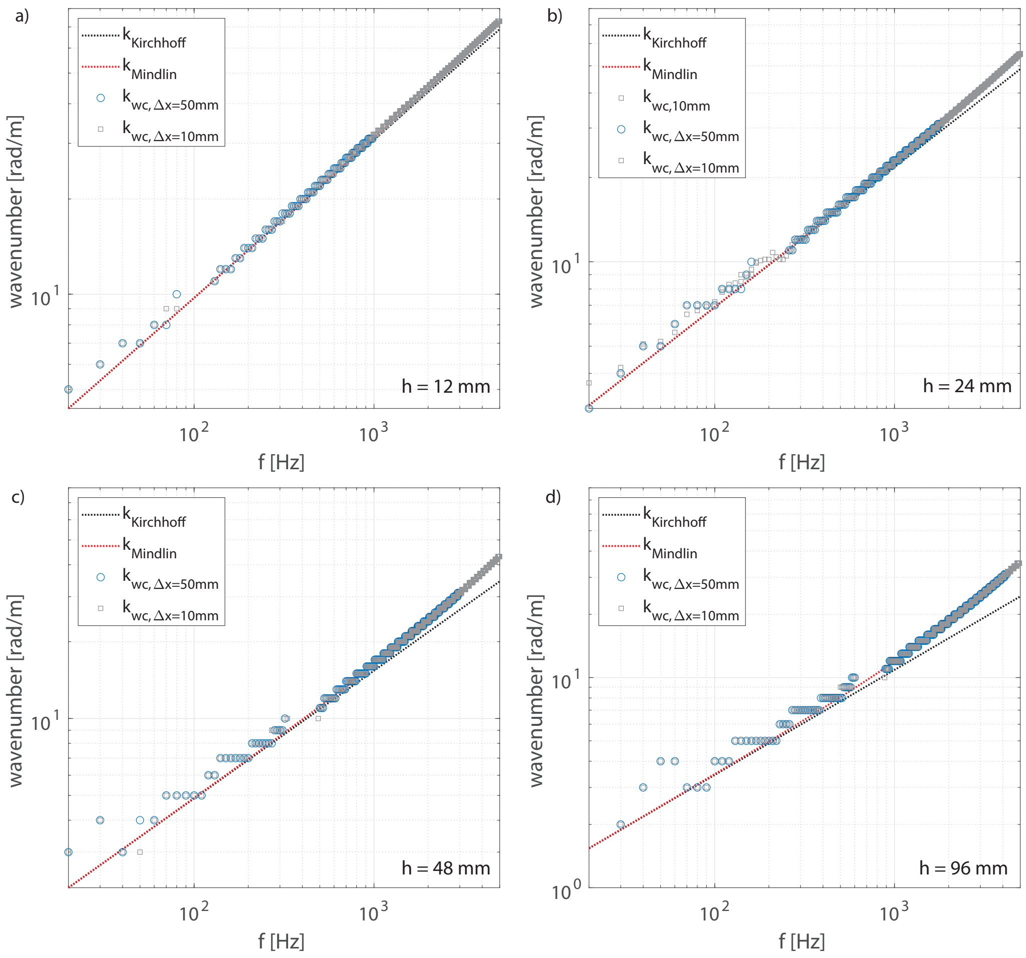

Figure 2: Benchmark results: comparison between the analytical wavenumber dispersion curves for thin and thick plates and the results obtained from a wave correlation approach applied to: a) 12 mm thick plasterboard; b) 24 mm thick plasterboard; c) 48 mm thick plasterboard; d) 96 mm thick plasterboard.

5. Experimental analysis

The measurements were performed in the Acoustic Laboratory of the Department of Industrial Engineering at the University of Bologna. A CLT floor was installed in the sound transmission test facilities with suppressed flanking transmission. The overall dimension of the floor is 4.44 x 2.82 m; it is made of four pieces of 5-plies 160 mm CLT elements (40/20/40/20/40), connected by fully threaded screws fixed with an angle of 45 degrees and sealed at the junctions. The

Table 1: Benchmark results: elastic properties of plasterboard element.

Method		E [GPa]	ϵ_E [%]	G [GPa]	ϵ_G [%]	FEM values E [GPa]	FEM values G [GPa]
ToF	Max Peak	2.93	4.8			2.80	1.08
	X-corr.	3.07	9.6				
	$\Delta\phi$	2.39	14.7				
	Kurtosis	2.62	6.3				
Wave Correlation	Kirch.h_{12mm}	2.30	17.9				
	Mindl.h_{12mm}	2.57	8.2	1.65	52.8		
	Kirch.h_{24mm}	1.92	31.4				
	Mindl.h_{24mm}	2.56	8.7	1.14	5.6		
	Kirch.h_{48mm}	1.45	48.1				
	Mindl.h_{48mm}	2.57	8.6	1.07	0.9		
	Kirch.h_{96mm}	0.98	67.5				
	Mindl.h_{96mm}	2.61	6.9	1.09	0.9		

floor is simply supported on the two longer edges and has free edges in the shorter dimension. The measurements that are presented in the paper refer to the principal direction parallel to grain, characterised by the higher bending stiffness. The density of the panel is ρ_{mean}= 420 kg/m^3; the Young's moduli parallel to grain and perpendicular to grain of each timber beam composing the layers are respectively $E_{0,mean}$= 12 GPa and $E_{90,mean}$= 0.37 GPa, while the shear modulus is G_{mean}= 0.69 GPa, as declared in the technical datasheet of the CLT panel.

The measurement setups used for the time domain methods and the frequency domain methods are different. A detailed description of the two procedures is provided below.

5.1. Time domain measurements

For the measurements in the time domain, the measurement equipment consisted of an electrodynamic shaker LDS V201 with an LDS PA25E power amplifier, an RME Fireface 802 soundcard, 1/2" ICP accelerometers (PCB Piezotronic) powered by a signal conditioner PCB Piezotronics 482C. For each investigated frequency, Gaussian-modulated sinusoidal pulses, gen-

Figure 3: Experimental setup used to investigate the CLT floor installed in the laboratory facility. a) side view: the shaker is mounted on a tripod with rubber supports on the three feet; b) top view: three accelerometers are mounted along a wave propagation direction in line with the excitation point.

erated in Matlab® for each investigated frequency, were run and recorded through REAPER® software, with a sampling frequency of 192 kHz. Two accelerometers were fixed to the floor using wax, at a mutual distance of 0.40 m along the strands of the face ply, as pictured in Figure 4. The pulses were centered at frequencies that ranged from 100 to 1500 Hz, with a step of 100 Hz. Each pulse was repeated 5 times. Measurements were done using three accelerometers at a time, and acquiring the input signal from an impedance head which was mounted on the shaker; this allowed to time-align all the measurements.

5.2. Frequency domain measurements

Measurements in the frequency domain were performed using the same electrodynamic shaker and accelerometers presented above. The measurements were controlled by means of

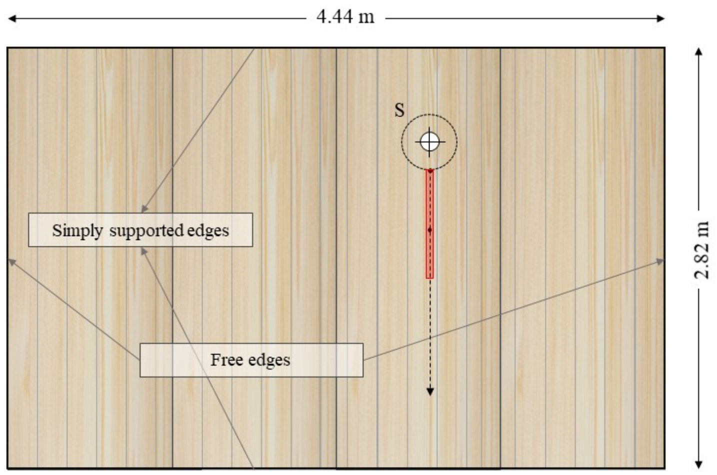

Figure 4: Scheme of the layout of the floor and the position of the accelerometers.

an in-house implemented LabVIEW software and the NI USB-4431 DAQ (data acquisition). Measurement positions spanned a total length of 0.72 m, the spacing between the accelerometers being 0.02 m. Also in this case, accelerometers were fixed to the floor using wax. The panel was excited driving the shaker with an exponential sine sweep. Each acquired signal was then convolved with the inverse filter of the sine sweep in order to obtain its impulse responses (IR), using a consolidated experimental technique [56]. The complex plate response spectra $s(\omega, x_i)$, measured over each point i, were obtained from the IR by means of a FFT algorithm. The acquisition of the signals was extremely fast, though limited by the number of accelerometers available which, with the given equipment, determined the maximum sampling frequency available for each channel.

6. Results and discussion

All the measurements were post-processed in Matlab®. Each signal was filtered using a low-pass filter to cancel high-frequency noise. Each method has specific settings that must be tweaked in order to bring the method to convergence.

In the analysis proposed, the maximum peak method is implemented by identifying the first relative maximum, to reduce the possibility of interference phenomena due to reflections. For each pulse, the prominence of the peaks was used as an input parameter to correctly detect the

Table 2: Estimate of the elastic modulus E and the shear modulus G from the non-linear fit performed using Mindlin's models.

Method	$E_{Mindlin}$ [GPa]	$G_{Mindlin}$ [GPa]
Maximum	3.37	0.300
Cross-correlation	2.48	0.280
Kurtosis	5.46	0.212
Phase difference	0.307	n. a.
Wave correlation	3.62	0.456

first peak. The results obtained from the kurtosis and the phase difference methods were strongly influenced by the width of the window and the length of the signal respectively.

The dispersion relations of the CLT plate obtained with the first four methods are reported in Figure 5. Using the first set of measurements (time domain pulses), a total of 5 measures were available for each frequency, as explained above. The results were then averaged and the standard deviation was calculated. These data were finally used to perform a non linear fit to Mindlin's model, based on the first order shear deformation plate theory. Although it can be argued that this theory neglects several high-order propagation modes, yet it is still one of the most used approaches implemented for vibro-acoustic prediction models, since it allows for a good approximation of the transverse displacement, which is the one of greatest importance to evaluate the fluid-structure interaction.

The raw data obtained by the application of the methods show that these measurements are affected by multiple reflections that are generated within the element. For most of the methods analysed, the dispersion of the data is relevant. The methods that provide lower dispersion of the data, frequency-by-frequency, are the maximum peak method and the cross-correlation method.

The results show that the method based upon the identification of the maximum peak provide the most consistent results in the whole frequency range of interest, with a limited dispersion of the data. A low variation was also found with the cross-correlation method. However, a good agreement between the fitted curve and the experimental data could be found only above 600 Hz, while at the lower frequencies high fluctuations were observed. The results obtained from

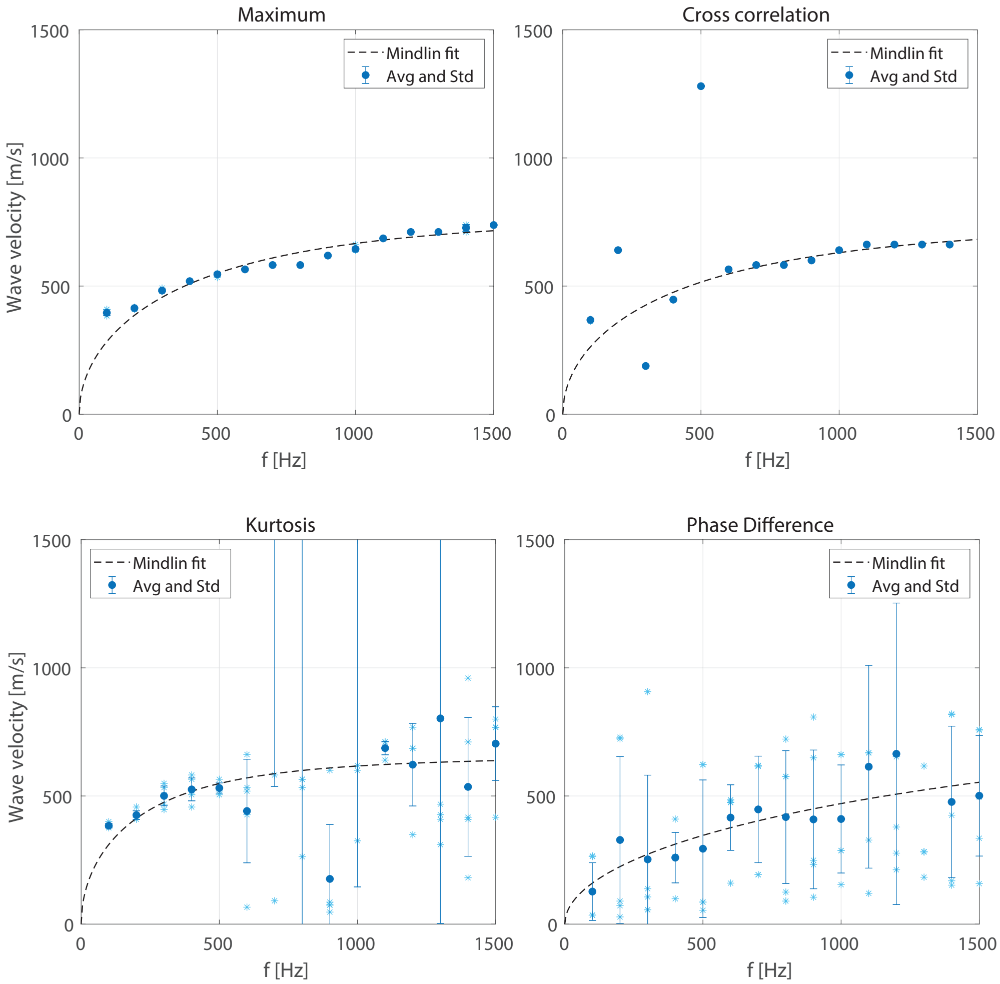

Figure 5: Measurement of bending waves velocity obtained with the four different methods based upon the acquisition of the pulses. Grey starred markers represent single measurements, while blue markers and bars represent the mean value and the standard deviation.

the kurtosis and the phase difference methods were characterised by a high deviation. While the kurtosis approach allowed to identify wave velocities consistent with the values obtained from the maximum-peak and the cross-correlation methods up to 500 Hz, the results determined with the phase difference method were characterised by high uncertainty within the entire frequency range.

The real part of the wavenumber determined with the wave correlation method is displayed in Figure 6. The graph on the left-hand side represents the real part of the function $\mathcal{F}$, given in Eq. 9, evaluated for a given value of the imaginary component of the wavenumber in the frequency range 0-3000 Hz. The maxima of the function are plotted using markers and were superimposed to the image. These points were then fitted using Mindlin's model, represented with a dashed red line. For a better readability, the experimental wavenumbers and the fitted curve are also reported in the right-hand side graph, with more suitable limits for the y-axis. The experimental wavenumber exhibited significant fluctuations in the lower frequency range, which is related to the evaluation length L_e over which the structure's dynamic response was measured. Moreover, in the range approximately between 1500 Hz and 2000 Hz the experimental wavenumbers seem to asymptotically flatten out. This behaviour, related to lateral reflections, could be misleading. In fact, higher wavenumbers were measured at higher frequencies. The possibility to investigate a broad frequency range allowed to perform a robust fitting with an analytic dispersion relation, even though experimental data exhibited fluctuations and high uncertainty in particular ranges of frequency.

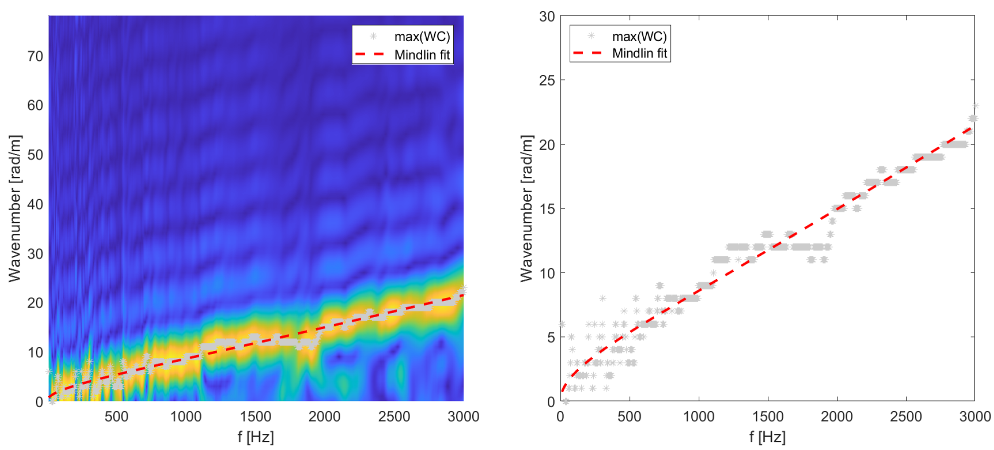

Figure 6: Dispersion image calculated with the wave correlation method: identification of the maxima to fit the dispersion relation (left) and estimate of the wave velocity (right).

For the five implemented methods, effective elastic and shear properties E and G were considered the optimisation variables of the non-linear fitting process, whereas Poisson's ratio was assumed to be a constant value of $\nu = 0.3$. The optimised variables obtained with each methods are summarised in Table 2. Moreover, in order to investigate the influence of the strong assumption made on the value of the Poisson ratio, a sensitivity analysis was conducted to estimate the effect that the hypothesised value of ν has on these quantities. To this aim, the wave correlation method was assumed as a reference and the experimental data were fitted with Mindlin's dispersion relation changing the value of the Poisson's ratio ν. The corresponding effective elastic properties E and G are then plotted on a two y-axes plot in Figure 7. Correlation between Poisson's ratio and E and G highlighted a non-linear relationship of these effective elastic properties over ν. By increasing the Poisson's ratio from $\nu = 0.1$ up to $\nu = 0.45$, a larger variation was found on $E(\nu = 0.45) \approx 0.8E(\nu = 0.1)$ rather than on $G(\nu = 0.45) \approx 0.9G(\nu = 0.1)$.

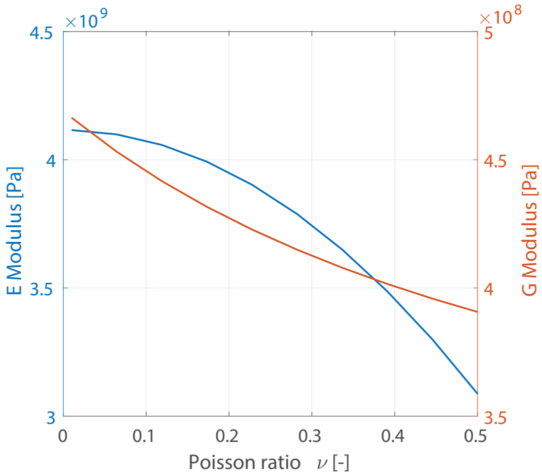

Figure 7: Sensitivity analysis of Poisson's ratio ν on the estimate of the elastic modulus E and on the shear modulus G.

The most intuitive approach to compare results obtained from methods for the characterisation of the elastic properties would be to compare the results with a target value, as done in Section 4. The data sheet of CLT elements provides the elastic properties of the lamellas which constitute each ply of the panel. Different methods can be found in the literature to estimate the equivalent Young modulus of a CLT element from the elastic properties of the timber lamellas and the number of plies of the panel [15]. Annex B of Eurocode 5 [57], for example, provides a method, based on the mechanically jointed beam theory, also known as Gamma Method. The values it provide can be used to perform structural analyses in static (or quasi-static) conditions. On the other hand, Mindlin's theory for thick plates was considered in this study, since it is widely used in vibro-acoustic analysis. It should be stressed that E and G are not the elastic constants of the CLT panel; rather, they represent apparent elastic properties to approximate the dynamic response of such a structure described as an equivalent homogeneous thick plate. The equivalent properties are suitable input data in homogenisation approaches as long as the assumptions made to derive them and the ones of the method of analysis are the same. For this reason, it is not possible to directly compare the elastic constants of the CLT panel derived by using the aforementioned methods, with the effective elastic properties determined in this study. Therefore, the investigated methods were compared in the following in terms of the wave velocity dispersion curves.

The comparison between methods based upon numerical input data showed an extremely good agreement under ideal conditions, the only limitations arising from physical problems (e.g. the Nyquist limit or transition from thin plate to thick plate behavior). Conversely, experimental measurements on a non-homogeneous plate are affected by a significantly larger variability. In Figure 8, the different methods are compared in terms of wave velocity determined for each investigated frequency. In particular, the graph on the left-hand side shows the experimental wave velocities directly determined from each method, or computed from the experimental wavenumbers. It is clear how all the methods are strongly affected by the complex structure on the CLT panel, generating multiple reflections in all the directions. However, some of them allow the identification of a certain trend while others totally fail to provide useful results to characterise wave propagation. The graph given on the right-hand side of Figure 8 shows the fitted dispersion curves calculated from the experimental data. The results obtained with the wave correlation are considered the most reliable, since they were fitted over a wider frequency range, up to 3000 Hz. The curve fitting of the experimental data obtained from the other methods, which only allowed the experimental investigation of a limited frequency range, was strongly influenced by the impossibility to correctly evaluate the effect of the shear deformations, which are significant above the shear wave crossover frequency, as defined in [37]. On the other hand, the frequency range of applicability of these methods could be extended by reducing the distance between the pair of transducers. Methods based on phase information are much more sensitive to the sensors spacing: several spacings should be considered to span the whole frequency range of interest. This consideration can be also a criterion to evaluate the efficiency of the use of one method compared to others. The wave correlation results provided clear information about wave propagation at the highest frequencies, and a trend which is in good agreement with the velocities obtained for the maximum-peak and the cross correlation methods up to 1500 Hz. In the graph on the right side of Figure 8, the curve labelled as *Maximum-WC* was obtained by fitting with Mindlin's dispersion relation a combined data set which considers the maximum-peak results up to 1500 and the wave correlation results from 1500 Hz up to 3000 Hz. This curve is in perfect agreement with the one obtained considering only the wave correlation based results, proving the reliability of this methods and the robustness of the curve fitting on the experimental data evaluated over an appropriate frequency range.

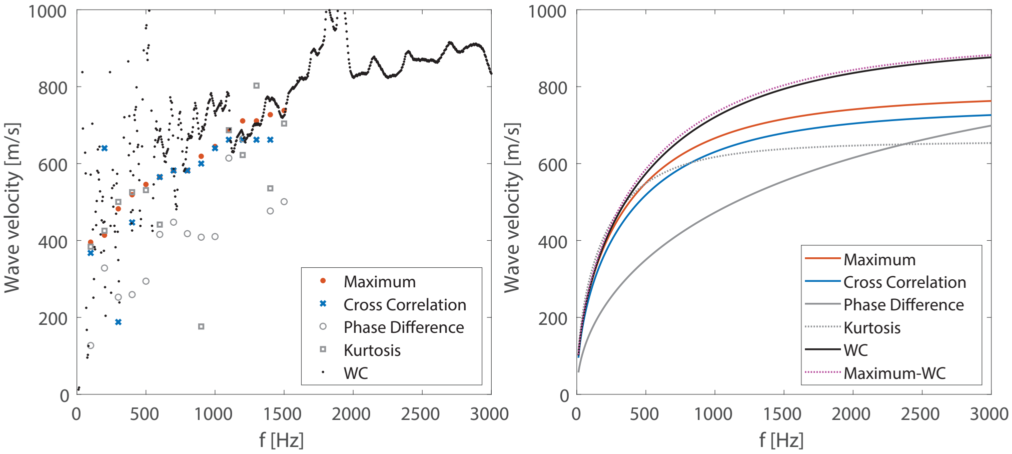

Figure 8: Wave velocity dispersion curves: experimental results determined with the five methods considered (left-hand side); curve fitting of the experimental data with Mindlin's dispersion relation (right-hand side).

It is finally worth comparing the performance of the methods considering the time required for the installation of each setup and for the gathering of the measures. The setup labelled in Section 5 as time-domain used three accelerometers at a time; a total of 16 frequencies were scanned, even though undersampling is possible, as discussed above. Each pulse was generated five times, for a total duration of 5 seconds each measurement (time interval of 1 sec between the pulses); since three measurement positions were considered for averaging, that leads to the processing of 80 signals. Conversely, frequency-domain measurements required a larger number of measurement positions, which can be performed also non-simultaneously, guaranteeing the same relative phase relationship with a reference transducer. The array used in this study consisted of 36 measurement points, performed using 3 accelerometers simultaneously. A 10 seconds sine sweep was averaged 5 times. The amount of time required to evaluate the structural dynamic response over an adequate length with a suitable spacing, is therefore dependent upon the availability of transducers and acquisition channels. The computational time required to run the algorithm is negligible compared to time required to perform the measurement.

Conclusions

The availability of an experimental estimate of the bending wavenumber is of great interest for vibro-acoustic modeling. Among the methods available in the literature, it is relevant to understand which methods are better suited to study different elements characterised by a peculiar dynamic response. The present study benchmarks methods for the extraction of dispersion relations on CLT elements, non homogeneous and orthotropic plates, focusing on the real component of the propagating wavenumber, from which apparent effective elastic properties could be evaluated, by means of a non-linear data fitting based on Mindlin's theory for thick plates. Five methods were selected, which are characterised by different experimental setups. They were first tested on an FE-simulated test signal; the results returned a good match between all results. Then, the methods were applied to signals measured on a CLT plate; here, the limitations characterizing each method emerged in relation to the sensitivity to background noise, to multiple reflections and to the ability to automatise the identification of optimal input parameters for a proper estimate. Among all methods tested, the maximum peak, implemented on the first relative maximum, the cross-correlation and the wave correlation method provided the most accurate results. Nevertheless, considering the time required for the measurement of the single pulses, the wave correlation method could be the most satisfactory method, given the availability of an array of transducers. This method, allowing to investigate a wider frequency range with a smaller computational effort, is useful for a proper estimate of an effective shear modulus G, which is strongly affected by the propagating wavenumer at mid-high frequencies. Reproducibility studies on CLT panels with different thickness and layer layup will be addressed in the future to verify the consistency of these results.

References

[1] A. Bukauskas, P. Mayencourt, P. Shepherd, B. Sharma, C. Mueller, P. Walker, J. Bregulla, Whole timber construction: A state of the art review, Construction and Building Materials 213 (2019) 748–769.

[2] F. Asdrubali, B. Ferracuti, L. Lombardi, C. Guattari, L. Evangelisti, G. Grazieschi, A review of structural, thermophysical, acoustical, and environmental properties of wooden materials for building applications, Building and Environment 114 (2017) 307–332.

[3] M. Caniato, F. Bettarello, A. Ferluga, L. Marsich, C. Schmid, P. Fausti, Thermal and acoustic performance expectations on timber buildings, Building Acoustics 24 (4) (2017) 219–237.

[4] A. Frangi, M. Fontana, E. Hugi, R. Jöbstl, Experimental analysis of cross-laminated timber panels in fire, Fire Safety Journal 44 (2009) 1078–1087.

[5] M. Izzi, D. Casagrande, S. Bezzi, D. Pasca, M. Follesa, R. Tomasi, Seismic behaviour of cross-laminated timber structures: A state-of-the-art review, Engineering Structures 170 (2018) 42–52.

[6] L. Muszynski, E. Hansen, S. Fernando, G. Schwarzmann, J. Rainer, Insights into the global cross-laminated timber industry, BioProducts Business 2 (8) (2017) 72–92.

[7] J. Lyslo Skullestad, R. A. Bohne, J. Lohne, High-rise timber buildings as a climate change mitigation measure - a comparative lca of structural system alternative, Energy Procedia 96 (2016) 112–123.

[8] M. H. Ramage, H. Burridge, M. Busse-Wicher, G. Fereday, T. Reynolds, D. U. Shah, G. Wu, L. Yu, P. Fleming, D. Densley-Tingley, J. Allwood, P. Dupree, P. Linden, O. Scherman, The wood from the trees: The use of timber in construction, Renewable and Sustainable Energy Reviews 68 (2017) 333–359.

[9] S. Ahmed, I. Arocho, Emission of particulate matters during construction: A comparative study on a cross laminated timber (CLT) and a steel building construction project, Journal of Building Engineering 22 (2019) 281–294.

[10] G. Íñiguez González, F. Arriaga, M. Esteban, D. F. Llana, Reference conditions and modification factors for the standardization of nondestructive variables used in the evaluation of existing timber structures, Construction and Building Materials 101 (2015) 1166–1171.

[11] J. H. Kurz, C. Boller, Some background of monitoring and NDT also useful for timber structures, Journal of Civil Structural Health Monitoring 5 (2015) 99–106.

[12] P. Palma, R. Steiger, Structural health monitoring of timber structures – Review of available methods and case studies, Construction and Building Materials 248 (2020) 118528.

[13] L. Zhang, A. Tiemann, T. Zhang, T. Gauthier, K. Hsu, M. Mahamid, P. Moniruzzaman, D. Ozevin, Nondestructive assessment of cross-laminated timber using non-contact transverse vibration and ultrasonic testing, European Journal of Wood and Wood Products (2021) 1–13.

[14] D. F. Llana, G. Íñiguez González, F. Arriaga, X. Wang, Time-of-flight adjustment procedure for acoustic measurements in structural timber, BioResources 11 (2) (2016) 3303–3317.

[15] J. Zhou, Y. H. Chui, M. Gong, L. Hu, Elastic properties of full-size mass timber panels: Characterization using modal testing and comparison with model predictions, Composites Part B 112 (2017) 203–212.

[16] A. Santoni, S. Schoenwald, B. Van Damme, P. Fausti, Determination of the elastic and stiffness characteristics of cross-laminated timber plates from flexural wave velocity measurements, Journal of Sound and Vibration 400 (2017) 387–401.

[17] A. Santoni, P. Bonfiglio, F. Mollica, P. Fausti, F. Pompoli, V. Mazzanti, Vibro-acoustic optimisation of wood plastic composite systems, Construction and Building Materials 174 (2018) 730–740.

[18] E. Nilsson, A. Nilsson, Prediction and measurement of some dynamic properties of sandwich structures with honeycomb and foam cores, Journal of sound and vibration 251 (3) (2002) 409–430.

[19] P. Margerit, A. Lebée, J.-F. Caron, X. Boutillon, High resolution wavenmber analysis (HRWA) for the mechanical characterisation of viscoelastic beams, Journal of Sound and Vibration 433 (2018) 198–211.

[20] F. Morandi, O. Robin, L. Barbaresi, M. Garai, N. Atalla, N. Quaegebeur, P. Masson, Benchmarking of methods for

the identification of flexural wavenumbers in wooden plates, in: Proceedings of the 23^{rd} International Congress on Acoustics, International Commission for Acoustics, Aachen, Germany, 2019.

[21] R. Steiger, A. Gülzow, C. Czaderski, M. T. Howald, P. Niemz, Comparison of bending stiffness of cross-laminated solid timber derived by modal analysis of full panels and by bending tests of strip-shaped specimens, European Journal of Wood and Wood Products 70 (1-3) (2012) 141–153.

[22] D. Gsell, G. Feltrin, S. Schubert, R. Steiger, M. Motavalli, Cross-laminated timber plates: Evaluation and verification of homogenized elastic properties, Journal of structural engineering 133 (1) (2007) 132–138.

[23] B. Van Damme, S. Schoenwald, A. Zemp, Modeling the bending vibration of cross-laminated timber beams, European Journal of Wood and Wood Products 75 (6) (2017) 985–994.

[24] B. Van Damme, A. Zemp, Measuring dispersion curves for bending waves in beams: A comparison of spatial fourier transform and inhomogeneous wave correlation, Acta Acustica united with Acustica 104 (2) (2018) 228–234.

[25] A. Thies, F. Morandi, L. Barbaresi, M. Garai, J. Hübelt, N. Kumer, Development of a quick and non-invasive measurement method for the extraction of the dispersion relation in CLT plates for the evaluation of the elastic parameters, in: Proceedings of the 23^{rd} International Congress on Acoustics, International Commission for Acoustics, Aachen, Germany, 2019.

[26] C. Qian, S. Ménard, D. Bard, J. Negreira, Development of a vibroacoustic stochastic finite element prediction tool for a clt floor, Applied Sciences 9 (6) (2019) 1106.

[27] T. Furtmüller, B. Giger, C. Adam, General shell section properties and failure model for cross-laminated timber obtained by numerical homogenization, Engineering Structures 163 (2018) 77–92.

[28] A. Santoni, P. Bonfiglio, P. Fausti, S. Schoenwald, Predicting sound radiation efficiency and sound transmission loss of orthotropic cross-laminated timber panels, in: Proceedings of Meetings on Acoustics, Acoustics'17, Vol. 30, ASA, EAA, 2017, p. 015013.

[29] A. Santoni, S. Schoenwald, P. Fausti, H. M. Tröbs, Modelling the radiation efficiency of orthotropic cross-laminated timber plates with simply-supported boundaries, Applied Acoustics 143 (2019) 112–124.

[30] R. Stürzenbecher, K. Hofstetter, J. Eberhardsteiner, Structural design of cross laminated timber (CLT) by advanced plate theories, Composites Science and Technology 70 (2010) 1368–1379.

[31] T. Furtmüller, C. Adam, Sound radiation of cross-laminated timber panels based on a higher order plate theory, Journal of Sound and Vibration 458 (2019) 335–346.

[32] Y. Yang, C. Fenemore, M. J. Kingan, B. R. Mace, Analysis of the vibroacoustic characteristics of cross laminated timber panels using a wave and finite element method, Journal of Sound and Vibration (2020) 115842.

[33] U. Arasan, F. Marchetti, F. Chevillotte, G. Tanner, D. Chronopoulos, E. Gourdon, On the accuracy limits of plate theories for vibro-acoustic predictions, Journal of Sound and Vibration 493 (2021) 115848.

[34] L. Cremer, M. Heckl, B. A. T. Petersson, Structure-borne sound, 3rd Edition, Springer-Verlag, Berlin Heidelberg, 2005.

[35] K. F. Graff, Wave motion in elastic solids, Dover Publications, Inc., New York, USA, 1991.

[36] I. A. Viktorov, Rayleigh and Lamb waves: physical theory and applications, Plenum Press, New York, USA, 1967.

[37] J. Rindel, Dispersion and absorption of structure-borne sound in acoustically thick plates, Applied Acoustics 41 (2) (1994) 97–111.

[38] M. Pearson, M. Eaton, C. Featherston, R. Pullin, K. Holford, Improved acoustic emission source location during fatigue and impact events in metallic and composite structures, Structural Health Monitoring 16(4) (2016) 1–18.

[39] R. Giannetti, A. Petrella, J. Bach, A. Silverman, Feasibility study of in vivo bone depth measurement using high frequency ultrasound, in: Instrumentation and Measurement Technology Conference (I2MTC), 2015 IEEE International, IEEE, 2015, pp. 762–766.

[40] J. M. Fresno, R. Giannetti, G. Robles, A survey of time-of-flight algorithms to determine bone positions in movement, in: 2017 IEEE International Instrumentation and Measurement Technology Conference (I2MTC), 2017, pp. 1–6.

[41] O. Khyam, S. Ge, X. Li, M. Pickering, Highly accurate time-of-flight measurement technique based on phase-correlation for ultrasonic ranging, IEEE Sensors Journal 17 (2) (2017) 434–443.

[42] C. Crispin, C. Mertens, Measurement of the bending stiffness of masonry walls by using time-frequeny analisys: Practical considerations and validation, in: Proceedings of the 23^{rd} International Congress on Acoustics, International Commission for Acoustics, Aachen, Germany, 2019.

[43] G. Robles, J. M. Fresno, R. Giannetti, Ultrasonic bone localization algorithm based on time-series cumulative kurtosis, ISA transactions 66 (2017) 469–475.

[44] G. Defrance, J.-D. Polack, Measuring the mixing time in auditoria, Journal of the Acoustical Society of America 123 (5) (2008) 3499.

[45] P. Bonfiglio, F. Pompoli, K. V. Horoshenkov, M. I. B. S. A. Rahim, L. Jaouen, J. Rodenas, F.-X. Bécot, E. Gourdon, D. Jaeger, V. Kursch, et al., How reproducible are methods to measure the dynamic viscoelastic properties of poroelastic media?, Journal of Sound and Vibration 428 (2018) 26–43.

[46] ASTM 756-05 – Standard Test Method for Measuring Vibration-Damping Properties of Materials., Standard, ASTM International, West Conshohocken, PA, USA (2010).

[47] A. Santoni, P. Bonfiglio, P. Fausti, F. Pompoli, Alternative method to the oberst technique to measure the complex elastic modulus of visco-elastic materials, Noise Control Engineering Journal 67 (1) (2019) 1–10.

[48] I. Roelens, F. Nuytten, I. Bosmans, G. Vermeir, In situ measurement of the stiffness properties of building components, Applied Acoustics 52 (3) (1997) 289–309.

[49] S. Conta, A. Santoni, A. Homb, Benchmarking the vibration velocity-based measurement methods to determine the radiated sound power from floor elements under impact excitation, Applied Acoustics 169 (2020) 107457.

[50] N. Roozen, L. Labelle, Q. Leclere, K. Ege, S. Alvarado, Non-contact experimental assessment of apparent dynamic stiffness of constrained-layer damping sandwich plates in a broad frequency range using a nd: Yag pump laser and a laser doppler vibrometer, Journal of Sound and Vibration 395 (2017) 90–101.

[51] J. Berthaut, M. Ichchou, L. Jezequel, K-space identification of apparent structural behaviour, Journal of Sound and Vibration 280 (3-5) (2005) 1125–1131.

[52] M. Ichchou, J. Berthaut, M. Collet, Multi-mode wave propagation in ribbed plates: Part i, wavenumber-space characteristics, International Journal of Solids and Structures 45 (5) (2008) 1179–1195.

[53] M. Ichchou, O. Bareille, J. Berthaut, Identification of effective sandwich structural properties via an inverse wave approach, Engineering Structures 30 (10) (2008) 2591–2604.

[54] J. Cuenca, F. Gautier, L. Simon, The image source method for calculating the vibrations of simply supported convex polygonal plates, Journal of Sound and vibration 322 (4-5) (2009) 1048–1069.

[55] N. Roozen, Q. Leclere, K. Ege, Y. Gerges, Estimation of plate material properties by means of a complex wavenumber fit using hankel's functions and the image source method, Journal of Sound and Vibration 390 (2017) 257–271.

[56] P. Guidorzi, L. Barbaresi, D. D'Orazio, M. Garai, Impulse responses measured with mls or swept-sine signals applied to architectural acoustics: an in-depth analysis of the two methods and some case studies of measurements inside theaters, Energy Procedia 78 (2015) 1611–1616.

[57] EN 1995-1-1:2014 – Eurocode 5: Design of timber structures – Part 1-1: General – Common rules and rules for buildings, Standard, European Committee for Standardization, Brussels, BE (2014).

Bozen, 10th July 2020

Declaration of Interest Statement

Manuscript title: "Determination of the dispersion relation in Cross-Laminated Timber plates: benchmarking of time- and frequency-domain methods."

Authors: Federica Morandi, Andrea Santoni, Patrizio Fausti, Massimo Garai

On behalf of the authors of this manuscript, I declare that the authors have no known competing financial interests or personal relationships that could have appeared to influence the work reported in this paper.

Sincerely,

Dr. Federica Morandi

MORANDI FEDERICA
10.07.2020
09:13:44 UTC

Author Agreement Statement

Manuscript title: "Determination of the dispersion relation in Cross-Laminated Timber plates: benchmarking of time- and frequency-domain methods."

Authors: Federica Morandi, Andrea Santoni, Patrizio Fausti, Massimo Garai

On behalf of the authors of this manuscript, I declare that this manuscript is original, has not been published before and is not currently being considered for publication elsewhere.
I confirm that the manuscript has been read and approved by all named authors and that there are no other persons who satisfied the criteria for authorship but are not listed. We further confirm that the order of authors listed in the manuscript has been approved by all of us. We understand that the Corresponding Author is the sole contact for the Editorial process. She is responsible for communicating with the other authors about progress, submissions of revisions and final approval of proofs

Sincerely,

Dr. Federica Morandi